Mechanics of Advanced Composite Structures 9 (2022) 317 – 334

Semnan University

Mechanics of Advanced Composite Structures

journal homepage: http://MACS.journals.semnan.ac.ir

Nonlinear Vibration of Rotating Laminated Composite Cross-ply Cylindrical Shell on Nonlinear Rotating Elastic Foundation

S. Mohammadrezazadeh *, A. A. Jafari

Faculty of Mechanical Engineering, K. N. Toosi University of Technology, Tehran, 19919 43344, Iran

KEYWORDS

Nonlinear vibration;
Rotating laminated composite cross-ply cylindrical shell;
Nonlinear rotating elastic foundation;
Modal analysis;
Multiple scales method.

ABSTRACT

This paper is focused on the study of nonlinear vibration of rotating laminated composite cross-ply cylindrical shells on a nonlinear rotating elastic foundation. In this study, FSDT is employed while the geometrical nonlinearity of the cylindrical shell is modeled considering the von Karman approach. It should be mentioned that this study is accomplished considering the influences of initial hoop tension as well as Coriolis and Centrifugal accelerations. The nonlinear equation of the rotating laminated composite cross-ply cylindrical shell is extracted via the Ritz method and then is written in the state space form. Then, modal analysis and the multiple scales method are applied to the nonlinear vibration equation in the state space form to obtain relations for nonlinear forward and backward frequency ratios. Validation of the results of this study is investigated considering some results published in the literature and good agreement is observed. Finally, the effects of the nonlinear and linear constants of the rotating foundation, radius, total thickness, length, and rotation speed on the linear frequencies, nonlinear parameters, and the curves of nonlinear frequency ratios versus amplitude parameters are acquired. The results show that the increase of the nonlinear constant of the rotating foundation doesn't influence the linear frequencies. Besides, linear frequencies increase with increase of the linear constants of the rotating elastic foundation and decrease with increase of the radius or total thickness. Furthermore, the increase of the nonlinear constant of the rotating elastic foundation or total thickness leads to an increase in nonlinear parameters and nonlinear frequency ratios. Conversely, the increase of the linear constants of the rotating foundation or the radius leads to a decrease in nonlinear parameters and frequency ratios. Moreover, the increase in amplitude parameters leads to an increase in the nonlinear frequency ratios.

1. Introduction

The vibration phenomenon is not suitable for many engineering structures and causes noise, fatigue, and failure [1]. Therefore, studying vibration behavior is substantial for the design of engineering structures. There are several researches in the literature which investigate the vibration or buckling of the structures. Sofiyev and Aksogan [2] investigated free vibration characteristics of thin non-homogeneous laminated orthotropic cylindrical shells considering geometric nonlinearity. Sofiyev et al. [3] carried out an investigation about the free vibration behavior of a thin laminated orthotropic non-homogeneous cylindrical shell surrounded by an elastic foundation taking into account the geometric nonlinearity. Najafov et al. [4] utilized the Karman-Donnell-type of kinematic nonlinearity, superposition principle, and Galerkin approach to study nonlinear free vibration of laminated orthotropic thin conical shells. Arshid et al. [5] investigated the buckling and bending of heterogeneous annular/circular micro sandwich plates resting on Pasternak substrate while electromagnetic fields and preloads are applied to the face sheets. Arshid and Khorshidvand [6] hired classical plate theory

* Corresponding author. Tel.: +98-21-88674747 ; Fax: +98-21-88674748
E-mail address: sh.mrezazadeh@gmail.com

DOI: 10.22075/macs.2022.23208.1337
Received 2021-04-20; Received in revised form 2021-08-14; Accepted 2022-08-27.

as well as the differential quadrature method to analyze the free vibration of a thin circular plate from a porous material integrated by piezoelectric actuator patches. Mohammadimehr et al. [7] hired third-order shear deformation shells theory and Hamilton principle to study magneto-electro-elastic vibration of functionally graded carbon nanotubes reinforced composites cylindrical shell under Electro-magnetic loads resting on visco-Pasternak elastic foundation. Babaei and Yang [8] handled an investigation about the longitudinal free vibration of a rotating rod on the basis of Eringen's nonlocal elasticity. Sofiyev [9] presented a review of the literature on the buckling and vibration of different types of functionally graded conical shells. Babaei et al. [10] studied the variations in the resonant frequency of a higher-order beam with the aid of Reddy-Levinson's theory considering rotation effects. Rahmani et al. [11] studied the lateral free vibration behavior of a micro-beam carrying a moveable attached mass. Avey and Yusufoglu [12] hired the nonlinear basic relations of von Karman as well as superposition, Galerkin, and semi-inverse methods to accomplish an investigation of the large amplitude vibration characteristics of carbon nanotube double-curved shallow shells. Arshid et al. [13] studied mechanical buckling and free vibration behavior of a three-layered curved microbeam subjected to the Lorentz magnetic load on the basis of the higher order shear deformation theory and Navier method. Khorasani et al. [14] investigated the thermo-elastic buckling treatment of a sandwich rectangular microplate surrounded by a Pasternak elastic foundation. Arshid and Amir [15] accomplished an investigation about the size-dependent vibration of three-layered fluid-infiltrated porous curved microbeams integrated with nanocomposite face sheets on an elastic foundation and subjected to thermal load. Mousavi et al. [16] focused on the free vibration study of a Porous Micro beam integrated with functionally graded piezoelectric layers with initial curvature with the aid of trigonometric shear deformation theories. Arshid et al. [17] investigated the thermal buckling behavior of annular/circular microplates resting on a Pasternak elastic foundation. Amir et al. investigated vibration characteristics of microbeams [18], microplates [19-21], and plates [22-23]. Arshid et al. investigated the vibration behavior of plates [24-26] and sandwich microplates [27]. Babaei [28-29] presented the longitudinal forced vibration response of nonlocal strain gradient rods.

Rotating cylindrical shells have numerous applications in industrial structures such as centrifugal separators and offshore drilling systems [30]. Reviewing the literature reveals that there are several works that focus on the vibration of rotating cylindrical shells [30-41]. Vibration with large amplitude requires the use of nonlinear simulation. A nonlinear simulation that is accomplished by consideration of nonlinear relations between strains and displacements is named geometrical nonlinearity [42]. There are several works in the literature that investigate about nonlinear vibration of rotating cylindrical shells. Young-Shin and Young-Wann [43] accomplished an investigation of the linear and nonlinear vibration of rotating hybrid cylindrical shells via the Ritz-Galerkin method. Liu and Chu [44] studied the nonlinear vibration behavior of clamped-free rotating thin cylindrical shells through Love thin shell theory and the Galerkin method. Wang [45] accomplished a study about the large amplitude vibration of a laminated composite rotating cylindrical shell subjected to radial harmonic excitation. Dong et al. [46] investigated linear and nonlinear vibration behaviors and dynamic responses of functionally graded graphene reinforced thin spinning cylindrical shells subjected to different boundary conditions and under static axial load via an analytical approach. Sun et al. [47] investigated nonlinear traveling wave vibration of thin simply supported rotating cylindrical shells with the Lagrange approach. Yao et al. [48] utilized a rotating pre-twisted cylindrical shell model to study the nonlinear dynamics of aero-engine compressor blades. Rostami et al. [49] employed first-order shear deformation theory and the Galerkin method to research about the nonlinear vibration and dynamic stability of sandwich rotating cylindrical shells. Liu et al. [50] investigated nonlinear breathing vibration of eccentric laminated composite rotating cylindrical shells subjected to temperature and lateral excitations using the Hamilton approach, Donnell theory, and the Galerkin method. Du et al. [51] used the Rayleigh-Ritz method, the domain decomposition approach, and the strain energy density principle to study nonlinear vibration characteristics of hard-coating rotating cylindrical shells subjected to radial harmonic excitations. Li et al. [52] employed Incremental Harmonic Balance Method and arc-length technique to study large-amplitude vibration of rotating thin laminated composite cylindrical shells subjected to arbitrary boundary conditions.

The cylindrical structure can rest on an elastic foundation and rotates with it. The Winkler-Pasternak model can be used for modeling the elastic foundation [53]. It should be noted that earthen soils can be modeled via the Pasternak model while sandy soils and liquids can be indicated by a model from Winkler [53 quoted

from 54-55]. It should be emphasized that generally the behavior of the foundation should be modeled in the nonlinear form [56]. Despite this fact, there are limited studies about the vibration of cylindrical structures on nonlinear elastic foundation. Sheng et al. [57] studied the nonlinear vibration behavior of functionally graded cylindrical shells on a nonlinear elastic medium via first-order shear deformation theory and the Galerkin technique. Sofiyev [58] dealt with the large amplitude vibration of orthotropic functionally graded cylindrical shells on the nonlinear elastic foundation with the help of Donnell's shell theory as well as the superposition and Galerkin techniques. Sofiyev and Kuruoglu [56] investigated the nonlinear dynamic behavior of heterogeneous orthotropic cylindrical shells surrounded by a nonlinear elastic foundation. Sofiyev et al. [59] presented nonlinear vibration of orthotropic cylindrical shells surrounded by nonlinear elastic foundations employing the shear deformation theory. Hadi et al. [60] handled the study of the nonlinear dynamics of functionally graded cylindrical shells resting on a nonlinear elastic foundation subjected to static and lateral dynamic loads in a thermal environment. Babaei et al. [61] employed higher order shear deformation shell theory, kinematic assumptions of Donnell and perturbation approach to study the vibration of long functionally graded material cylindrical panel on a nonlinear foundation.

It seems from the literature review that there is not any investigation of the nonlinear vibration of rotating cylindrical shells on a nonlinear rotating foundation. Thus, in this study, an impressive approach that converts nonlinear equation of the system to state space form and applies modal analysis and multiple scales method is used to study the nonlinear vibration of laminated composite rotating cylindrical shells on a nonlinear rotating elastic foundation. It is required to mention that the Winkler-Pasternak model is used to model the rotating elastic foundation surrounding the rotating cylindrical shell. It should be mentioned that the rotation speeds of the shell and foundation are the same. First-order shear deformation theory (FSDT) considering the effect of rotary inertia is employed to obtain the vibration equation of the shell while geometrical nonlinearity is modeled with von Karman's theory. The nonlinear vibration equation of the rotating cylindrical shell is derived considering the effects of initial hoop tension as well as Coriolis and centrifugal accelerations. In order to derive a nonlinear differential equation of the vibration, the Ritz method is considered. Then, the responses for nonlinear forward and backward frequency ratios are extracted via a method that is a compound of modal analysis and multiple scales approach while the state space form of the vibration equation is considered. Some results of this study are compared with published literature to confirm the validity of this study. In the next step, the study about the effects of the nonlinear and linear coefficients of the rotating elastic foundation, radius, total thickness, length, and rotation speed on the linear frequencies, nonlinear parameters, and curves of amplitude parameter versus nonlinear frequency ratio for both forward and backward waves is accomplished.

2. Problem Formulation

In this study, a laminated composite cylindrical shell that rotates with constant Ω rotation speed and is on the nonlinear rotating elastic foundation is considered. The length of this shell is shown with L, its radius is exhibited with R while h is used to demonstrate the total thickness. The considered rotating cylindrical shell is cross-ply with lamination scheme of $[90^o/0^o/90^o]_s$. A schematic image of this shell with a coordinate system and elastic foundation is shown in Fig 1. It should be noted that s, β and z indicate longitudinal, circumferential, and normal directions of the coordinate system, respectively.

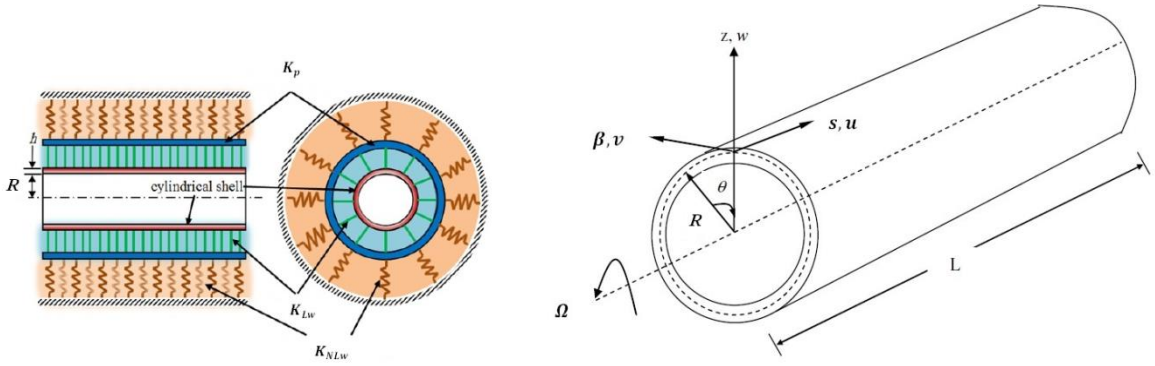

Fig. 1. Schematic of the rotating cylindrical shell placed on nonlinear rotating elastic foundation used in this study [35, 60]

In order to obtain strains of the shell, considering FSDT and the nonlinear von Karman approach lead to the extraction of the following relations [62-63]:

$$\begin{aligned}
&\varepsilon_s = \varepsilon_{0s} + zk_s, \quad \varepsilon_\beta = \varepsilon_{0\beta} + zk_\beta, \\
&\varepsilon_{s\beta} = \varepsilon_{0s\beta} + zk_{s\beta} \\
&\varepsilon_{sz} = \frac{\partial w_0}{\partial s} + \psi_s, \quad \varepsilon_{\beta z} = \frac{1}{R}\frac{\partial w_0}{\partial \beta} - \frac{v_0}{R} + \psi_\beta
\end{aligned} \tag{1}$$

$$\begin{aligned}
&\varepsilon_{0s} = \frac{\partial u_0}{\partial s} + \frac{1}{2}\left(\frac{\partial w_0}{\partial s}\right)^2, \\
&\varepsilon_{0\beta} = \frac{1}{R}\frac{\partial v_0}{\partial \beta} + \frac{w_0}{R} + \frac{1}{2R^2}\left(\frac{\partial w_0}{\partial \beta}\right)^2, \\
&\varepsilon_{0s\beta} = \frac{\partial v_0}{\partial s} + \frac{1}{R}\frac{\partial u_0}{\partial \beta} + \frac{1}{R}\frac{\partial w_0}{\partial s}\frac{\partial w_0}{\partial \beta}, \\
&k_s = \frac{\partial \psi_s}{\partial s}, \quad k_\beta = \frac{1}{R}\frac{\partial \psi_\beta}{\partial \beta}, \\
&k_{s\beta} = \frac{\partial \psi_\beta}{\partial s} + \frac{1}{R}\frac{\partial \psi_s}{\partial \beta}
\end{aligned} \tag{2}$$

while u_0, v_0 and w_0 demonstrating displacements of a point on mid-surface along s, β and z directions, respectively [62]. It should be mentioned that in equations (1) and (2), ψ_s and ψ_β are respectively total angular rotations of the normal to mid-surface about β and s axes [62]. In order to obtain in-plane forces (N_s, N_β, $N_{s\beta}$), moments (M_s, M_β, $M_{s\beta}$), as well as transverse forces (Q_s, Q_β) for cross-ply rotating cylindrical shells, equation (3), can be utilized [63]:

$$\begin{aligned}
&\begin{Bmatrix} N_s \\ N_\beta \end{Bmatrix} = \begin{bmatrix} A_{11} & A_{12} \\ A_{12} & A_{22} \end{bmatrix} \begin{Bmatrix} \varepsilon_{0s} \\ \varepsilon_{0\beta} \end{Bmatrix}, \\
&\begin{Bmatrix} M_s \\ M_\beta \end{Bmatrix} = \begin{bmatrix} D_{11} & D_{12} \\ D_{12} & D_{22} \end{bmatrix} \begin{Bmatrix} k_s \\ k_\beta \end{Bmatrix} \\
&N_{s\beta} = A_{66}\varepsilon_{0s\beta}, \quad M_{s\beta} = D_{66}k_{s\beta}, \\
&Q_s = \frac{5}{6}A_{55}\varepsilon_{sz}, \quad Q_\beta = \frac{5}{6}A_{44}\varepsilon_{\beta z}
\end{aligned} \tag{3}$$

while [63]:

$$\begin{aligned}
&A_{ij} = \int_z \bar{Q}_{ij}dz, \quad D_{ab} = \int_z \bar{Q}_{ij}z^2 dz, \\
&ij = 11,12,22,66,44,55 \\
&ab = 11,12,22,66
\end{aligned} \tag{4}$$

while $\bar{Q}_{ij}$ denote transformed plane-stress-reduced stiffnesses [63].

3. Hamilton Principle and Ritz Method

In order to obtain the results of this study with the Ritz method [63, 64], it is requested to use the variational form of the Hamilton principle [62, 65] which is as follows for the problem of this study:

$$\int_t \left(\delta T - \delta U_\varepsilon - \delta U_h - \delta U_k\right)dt = 0 \tag{5}$$

while t [62] is used to demonstrate the time variable and T [62, 65] and U_ε [62] denote kinetic and strain energies, respectively, with the following variational formulations:

$$\begin{aligned}
\delta T &= \int_\beta \int_s -I_1 \ddot{u}_0 \delta u_0 R ds d\beta \\
&+ \int_\beta \int_s I_1(\Omega^2 v_0 - \ddot{v}_0 - 2\Omega \dot{w}_0)\delta v_0 R ds d\beta \\
&+ \int_\beta \int_s I_1(\Omega^2 w_0 + 2\Omega \dot{v}_0 - \ddot{w}_0)\delta w_0 R ds d\beta \\
&+ \int_\beta \int_s I_2(-\ddot{\psi}_s \delta u_0 - \ddot{u}_0 \delta \psi_s + 2\Omega \dot{\psi}_\beta \delta w_0) R ds d\beta \\
&+ \int_\beta \int_s I_2(\Omega^2 \psi_\beta - \ddot{\psi}_\beta)\delta v_0 R ds d\beta \\
&+ \int_\beta \int_s I_2(\Omega^2 v_0 - \ddot{v}_0 - 2\Omega \dot{w}_0)\delta \psi_\beta) R ds d\beta \\
&+ \int_\beta \int_s I_3(-\ddot{\psi}_s \delta \psi_s + (\Omega^2 \psi_\beta - \ddot{\psi}_\beta)\delta \psi_\beta) R ds d\beta
\end{aligned} \tag{6}$$

$$\begin{aligned}
\delta U_\varepsilon &= \int_s \int_\beta N_s \left(\frac{\partial \delta u_0}{\partial s} + \frac{\partial w_0}{\partial s}\frac{\partial \delta w_0}{\partial s}\right) R d\beta ds \\
&+ \int_s \int_\beta N_\beta \left(\frac{\partial \delta v_0}{\partial \beta} + \delta w_0 + \frac{1}{R}\frac{\partial w_0}{\partial \beta}\frac{\partial \delta w_0}{\partial \beta}\right) d\beta ds \\
&+ \int_s \int_\beta M_s \frac{\partial \delta \psi_s}{\partial s} R d\beta ds \\
&+ \int_s \int_\beta N_{s\beta} \left(\frac{\partial \delta v_0}{\partial s} + \frac{1}{R}\frac{\partial \delta u_0}{\partial \beta}\right) R d\beta ds \\
&+ \int_s \int_\beta N_{s\beta} \left(\frac{\partial \delta w_0}{\partial s}\frac{\partial w_0}{\partial \beta} + \frac{\partial w_0}{\partial s}\frac{\partial \delta w_0}{\partial \beta}\right) d\beta ds \\
&+ \int_s \int_\beta M_\beta \frac{\partial \delta \psi_\beta}{\partial \beta} d\beta ds \\
&+ \int_s \int_\beta M_{s\beta} \left(\frac{\partial \delta \psi_\beta}{\partial s} + \frac{1}{R}\frac{\partial \delta \psi_s}{\partial \beta}\right) R d\beta ds \\
&+ \int_s \int_\beta Q_s \left(\frac{\partial \delta w_0}{\partial s} + \delta \psi_s\right) R d\beta ds \\
&+ \int_s \int_\beta Q_\beta \left(\frac{\partial \delta w_0}{\partial \beta} - \delta v_0 + R\,\delta \psi_\beta\right) d\beta ds
\end{aligned} \tag{7}$$

The terms of equation (6) are related to Ω^2 and 2Ω are dependent on centrifugal and Coriolis accelerations, respectively. In addition, the inertia terms of equation (6) can be determined by equation (8) [66]:

$$I_1=\sum_{k=1}^{N}\int_z \rho^{(k)}dz\ ,\quad I_2=\sum_{k=1}^{N}\int_z \rho^{(k)}zdz\ ,$$
$$I_3=\sum_{k=1}^{N}\int_z \rho^{(k)}z^{2}dz \tag{8}$$

while the term $\rho^{(k)}$ demonstrates mass density of the kth layer [66] of the rotating laminated composite cylindrical shell. In equation (5), U_h shows the energy caused due to the initial hoop tension ($N_\beta^{\ 0}=I_1R^2\Omega^2$) [47]:

$$U_h=\int_s\int_\beta \frac{N_\beta^{\ 0}}{2R}\begin{pmatrix}\left(\frac{\partial u_0}{\partial\beta}\right)^2+\left(\frac{\partial v_0}{\partial\beta}+w_0\right)^2\\+\left(v_0-\frac{\partial w_0}{\partial\beta}\right)^2\end{pmatrix}d\beta ds \tag{9}$$

In equation (5), the term δU_k refers to the variational form of the energy caused due to the elastic foundation [56]:

$$\delta U_k=\int_s\int_\beta (K_{Lw}w_0+K_{NLw}w_0^{\ 3})R\,\delta w_0 d\beta ds$$
$$-\int_s\int_\beta K_p\left(\frac{\partial^2 w_0}{\partial s^2}+\frac{1}{R^2}\frac{\partial^2 w_0}{\partial\beta^2}\right)R\,\delta w_0 d\beta ds \tag{10}$$

whereas K_{Lw} and K_{NLw} denote linear and nonlinear coefficients of Winkler elastic foundation, respectively [56]. Furthermore, K_p indicate the shear stiffness of the foundation [56]. In order to use the Ritz method, it is required to choose approximation functions that satisfy geometrical boundary conditions [63] which are as $v(s,\beta,z)=0, w(s,\beta,z)=0, \psi_\beta(s,\beta,z)=0$, $s=0$, L for rotating cylindrical shells which are simply supported at two ends [66]. In this way, the following relation can be considered for rotating laminated composite simply supported cylindrical shells:

$$\begin{aligned}
u_0&=\cos\frac{m\pi s}{L}\left(u_{t1}(t)\cos n\beta-u_{t2}(t)\sin n\beta\right)\\
v_0&=\sin\frac{m\pi s}{L}\left(v_{t1}(t)\sin n\beta+v_{t2}(t)\cos n\beta\right)\\
w_0&=\sin\frac{m\pi s}{L}\left(w_{t1}(t)\cos n\beta-w_{t2}(t)\sin n\beta\right)\\
\psi_s&=\cos\frac{m\pi s}{L}\left(\psi_{st1}(t)\cos n\beta-\psi_{st2}(t)\sin n\beta\right)\\
\psi_\beta&=\sin\frac{m\pi s}{L}\left(\psi_{\beta t1}(t)\sin n\beta+\psi_{\beta t2}(t)\cos n\beta\right)
\end{aligned} \tag{11}$$

while $m,n=1,2,\ldots$. It is necessary to mention that in equation (11), the relations for u_0 , v_0 and w_0 are written based on reference [47]. It is supposed that initial conditions are in a form that equation (11) can satisfy them. Substituting equation (11) into equations (6), (7), (9) and (10) and then substituting the results in equation (5) and performing required integrals and simplifications lead to the nonlinear ordinary differential equation of the system as follows:

$$\mathbf{M}\ddot{\mathbf{x}}+\mathbf{C}\dot{\mathbf{x}}+\mathbf{K}\mathbf{x}+\mathbf{g}_1w_{t1}^{\ 3}+\mathbf{g}_2w_{t2}^{\ 3}+\mathbf{g}_3w_{t1}w_{t2}^{\ 2}$$
$$+\mathbf{g}_4w_{t2}w_{t1}^{\ 2}=\mathbf{0} \tag{12}$$

In equation (12), $\mathbf{M}$ and $\mathbf{K}$ exhibit mass and stiffness matrices, respectively. It is notable to express that matrix $\mathbf{K}$ contains terms related to stiffness, centrifugal acceleration, and initial hoop tension. Besides, the matrix $\mathbf{C}$ contains components established due to Coriolis acceleration caused by rotation of the shell and also:

$$\mathbf{x}=\left\{u_{t1},u_{t2},v_{t1},v_{t2},w_{t1},w_{t2},\psi_{st1},\psi_{st2},\psi_{\beta t1},\psi_{\beta t2}\right\}^T \tag{13}$$

Linearization of equation (12) around zero equilibrium point leads to the equation $\mathbf{M}\ddot{\mathbf{x}}+\mathbf{C}\dot{\mathbf{x}}+\mathbf{K}\mathbf{x}=\mathbf{0}$. The smallest frequency that corresponds to the equation $\mathbf{M}\ddot{\mathbf{x}}+\mathbf{C}\dot{\mathbf{x}}+\mathbf{K}\mathbf{x}=\mathbf{0}$ is called forward linear frequency. It can be generally claimed that the absolute value of backward frequency is greater than the absolute value of forward frequency [67]. Thus, the frequency which is greater than forward linear frequency and smaller than other frequencies is called backward linear frequency. It should be emphasized that the components of the matrix $\mathbf{C}$ lead to obtaining forward and backward frequencies.

4. Obtain the Responses

In this section of the paper, the nonlinear responses for both forward and backward waves are obtained. In this way, in the first step, equation (12) is written in the state space form [62] as follows:

$$\dot{\mathbf{y}}=\mathbf{A}\mathbf{y}+\mathbf{g}_5w_{t1}^{\ 3}+\mathbf{g}_6w_{t2}^{\ 3}+\mathbf{g}_7w_{t1}w_{t2}^{\ 2}$$
$$+\mathbf{g}_8w_{t2}w_{t1}^{\ 2} \tag{14}$$

while:

$$\mathbf{y}=\begin{Bmatrix}\mathbf{x}\\ \dot{\mathbf{x}}\end{Bmatrix},\quad \mathbf{A}=\begin{bmatrix}\mathbf{0} & \mathbf{I}(10,10)\\ -\mathbf{M}^{-1}\mathbf{K} & -\mathbf{M}^{-1}\mathbf{C}\end{bmatrix}, \tag{15}$$

$\mathbf{I}(10,10)$ is unit matrix.

$$\mathbf{g}_5=\begin{Bmatrix}\mathbf{0}\\ -\mathbf{M}^{-1}\mathbf{g}_1\end{Bmatrix},\quad \mathbf{g}_6=\begin{Bmatrix}\mathbf{0}\\ -\mathbf{M}^{-1}\mathbf{g}_2\end{Bmatrix},$$
$$\mathbf{g}_7=\begin{Bmatrix}\mathbf{0}\\ -\mathbf{M}^{-1}\mathbf{g}_3\end{Bmatrix},\quad \mathbf{g}_8=\begin{Bmatrix}\mathbf{0}\\ -\mathbf{M}^{-1}\mathbf{g}_4\end{Bmatrix} \tag{16}$$

In order to obtain solutions of equation (14), one can use the multiple scales method [68] which is an impressive method for the solution of nonlinear ordinary differential equations. In order to use this method with $O(\varepsilon^3)$ approximation, one must rewrite the nonlinear time t related differential equation (14) in the form of a partial differential equation related to $T_0=t$, $T_1=\varepsilon t$ and $T_2=\varepsilon^2 t$ while ε denotes a

small dimensionless parameter [68]. Furthermore, it is required to write $\mathbf{y}$, w_{t1} and w_{t2} as functions of newly defined variables T_0, T_1 and T_2; thus the terms of $\mathbf{y}$, $\dot{\mathbf{y}}$ and also w_{t1} and w_{t2} which are coefficients of $\varepsilon^n, n=1,2,3$ can be written in the following types [68]:

$$\mathbf{y}(t)=\varepsilon\mathbf{y_1}(T_0,T_1,T_2)+\varepsilon^2\mathbf{y_2}(T_0,T_1,T_2)+\varepsilon^3\mathbf{y_3}(T_0,T_1,T_2) \tag{17}$$

$$\dot{\mathbf{y}}=\varepsilon\left(D_0\mathbf{y_1}+\varepsilon D_1\mathbf{y_1}+\varepsilon^2 D_2\mathbf{y_1}\right)+\varepsilon^2\left(D_0\mathbf{y_2}+\varepsilon D_1\mathbf{y_2}\right)+\varepsilon^3 D_0\mathbf{y_3} \tag{18}$$

$$w_{t1}(t)=\varepsilon w_{11}(T_0,T_1,T_2)+\varepsilon^2 w_{12}(T_0,T_1,T_2)+\varepsilon^3 w_{13}(T_0,T_1,T_2) \tag{19}$$

$$w_{t2}(t)=\varepsilon w_{21}(T_0,T_1,T_2)+\varepsilon^2 w_{22}(T_0,T_1,T_2)+\varepsilon^3 w_{23}(T_0,T_1,T_2) \tag{20}$$

while $D_0=\partial/\partial T_0$, $D_1=\partial/\partial T_1$ and $D_2=\partial/\partial T_2$. Substituting equations (17) to (20) into equation (14) and some simplifications lead to an equation that contains terms which are coefficients of ε, ε^2 and ε^3. One can obtain the following relations by considering the coefficients of ε, ε^2 and ε^3 in the obtained equation equal to zero:

$$\varepsilon \Rightarrow D_0\mathbf{y_1}-\mathbf{A}\mathbf{y_1}=\mathbf{0} \tag{21}$$

$$\varepsilon^2 \Rightarrow D_0\mathbf{y_2}-\mathbf{A}\mathbf{y_2}=-D_1\mathbf{y_1} \tag{22}$$

$$\varepsilon^3 \Rightarrow D_0\mathbf{y_3}-\mathbf{A}\mathbf{y_3}=-D_1\mathbf{y_2}-D_2\mathbf{y_1}+\mathbf{g_5}w_{11}{}^3+\mathbf{g_6}w_{21}{}^3+\mathbf{g_7}w_{11}w_{21}{}^2+\mathbf{g_8}w_{21}w_{11}{}^2 \tag{23}$$

In order to find the solution of equation (21), using modal analysis relation $\mathbf{y_1}=\mathbf{Y}\{\eta_1\}$ [62] leads to the following relation:

$$\{D_0\eta_1\}=[\lambda_i]\{\eta_1\},\ [\lambda_i]=\left(\mathbf{Z}^T\mathbf{Y}\right)^{-1}\mathbf{Z}^T\mathbf{A}\mathbf{Y} \tag{24}$$

It is important to mention that $\mathbf{Y}$ and $\mathbf{Z}$ refer to matrices of right and left eigenvectors, respectively, while $\{\eta_1\}$ demonstrates modal coordinates vector [62]. Two rows in equation (24) include forward linear frequency (ω_f); also, two rows of the relation (24) contain backward linear frequency (ω_b). The responses of the rows of equation (24) which contain forward or backward linear frequencies are derived using equations (25) and (26), respectively:

$$\eta_{1f1}=\eta_1(f_1,1)=\mathbf{a_f}\exp(i\,\omega_f T_0),\quad \eta_{1f2}=\eta_1(f_2,1)=\bar{\mathbf{a}}_\mathbf{f}\exp(-i\,\omega_f T_0) \tag{25}$$

$$\eta_{1b1}=\eta_1(b_1,1)=\mathbf{a_b}\exp(i\,\omega_b T_0),\quad \eta_{1b2}=\eta_1(b_2,1)=\bar{\mathbf{a}}_\mathbf{b}\exp(-i\,\omega_b T_0) \tag{26}$$

while subscripts f and b indicate forward and backward waves of the rotating laminated composite cylindrical shell, respectively. Substituting modal analysis relations $\mathbf{y_1}=\mathbf{Y}\{\eta_1\}$ and $\mathbf{y_2}=\mathbf{Y}\{\eta_2\}$ [62] into equation (22) and some simplifications lead to:

$$\{D_0\eta_2\}=[\lambda_i]\{\eta_2\}+\mathbf{P}\{D_1\eta_1\},\quad [\lambda_i]=\left(\mathbf{Z}^T\mathbf{Y}\right)^{-1}\mathbf{Z}^T\mathbf{A}\mathbf{Y},\ \ \mathbf{P}=-\left(\mathbf{Z}^T\mathbf{Y}\right)^{-1}\mathbf{Z}^T\mathbf{Y} \tag{27}$$
$$\Rightarrow\{D_1\eta_1\}=\mathbf{0}\Rightarrow\{\eta_1(T_2)\}$$

Thus the particular solution of equation (27) is $\{\eta_2\}=\mathbf{0}$. It should be noted that in addition to $\{\eta_1\}$, $\{\eta_2\}$ also indicates the vector of modal coordinates [62]. Substituting $\{\eta_2\}=\mathbf{0}$, modal analysis relations $\mathbf{y_3}=\mathbf{Y}\{\eta_3\}$ and $\mathbf{y_1}=\mathbf{Y}\{\eta_1\}$ [62] into equation (23) and performing some mathematical efforts, one can acquire the following relation:

$$\{D_0\eta_3\}=[\lambda_i]\{\eta_3\}+\mathbf{P}\{D_2\eta_1\}+\hat{\mathbf{g}}_5 w_{11}{}^3+\hat{\mathbf{g}}_6 w_{21}{}^3+\hat{\mathbf{g}}_7 w_{11}w_{21}{}^2+\hat{\mathbf{g}}_8 w_{21}w_{11}{}^2 \tag{28}$$

while:

$$\hat{\mathbf{g}}_5=\left(\mathbf{Z}^T\mathbf{Y}\right)^{-1}\mathbf{Z}^T\mathbf{g}_5,\ \ \hat{\mathbf{g}}_6=\left(\mathbf{Z}^T\mathbf{Y}\right)^{-1}\mathbf{Z}^T\mathbf{g}_6,\quad \hat{\mathbf{g}}_7=\left(\mathbf{Z}^T\mathbf{Y}\right)^{-1}\mathbf{Z}^T\mathbf{g}_7,\ \ \hat{\mathbf{g}}_8=\left(\mathbf{Z}^T\mathbf{Y}\right)^{-1}\mathbf{Z}^T\mathbf{g}_8 \tag{29}$$

Considering the row of equation (28) which contains linear forward frequency and neglecting all frequencies other than linear forward frequency, leads to the following relation:

$$D_0\eta_{3f1}=\lambda_f\eta_{3f1}-D_2\eta_{1f1}-D_2\eta_{1f2}+q_{1f}\eta_{1f1}{}^3+q_{2f}\eta_{1f2}{}^3+q_{3f}\eta_{1f1}{}^2\eta_{1f2}+q_{4f}\eta_{1f1}\eta_{1f2}{}^2 \tag{30}$$

where in:

$$\begin{aligned}
q_{1f}&=\hat{g}_{5f1}Y_{5f1}{}^3+\hat{g}_{6f1}Y_{6f1}{}^3+\hat{g}_{7f1}Y_{6f1}{}^2Y_{5f1}+\hat{g}_{8f1}Y_{5f1}{}^2Y_{6f1}\\
q_{2f}&=\hat{g}_{5f1}Y_{5f2}{}^3+\hat{g}_{6f1}Y_{6f2}{}^3+\hat{g}_{7f1}Y_{6f2}{}^2Y_{5f2}+\hat{g}_{8f1}Y_{5f2}{}^2Y_{6f2}\\
q_{3f}&=3\hat{g}_{5f1}Y_{5f2}Y_{5f1}{}^2+3\hat{g}_{6f1}Y_{6f2}Y_{6f1}{}^2+2\hat{g}_{7f1}Y_{6f1}Y_{6f2}Y_{5f1}+\hat{g}_{7f1}Y_{6f1}{}^2Y_{5f2}\\
&\quad+2\hat{g}_{8f1}Y_{5f1}Y_{5f2}Y_{6f1}+\hat{g}_{8f1}Y_{5f1}{}^2Y_{6f2}\\
q_{4f}&=3\hat{g}_{5f1}Y_{5f2}{}^2Y_{5f1}+3\hat{g}_{6f1}Y_{6f2}{}^2Y_{6f1}+\hat{g}_{7f1}Y_{6f2}{}^2Y_{5f1}+2\hat{g}_{7f1}Y_{6f1}Y_{6f2}Y_{5f2}\\
&\quad+\hat{g}_{8f1}Y_{5f2}{}^2Y_{6f1}+2\hat{g}_{8f1}Y_{5f1}Y_{5f2}Y_{6f2}
\end{aligned} \tag{31}$$

$$\begin{aligned}&\hat{g}_{5f\,1}=\hat{\mathbf{g}}_{\mathbf{5}}(f_1,1),\quad \hat{g}_{6f\,1}=\hat{\mathbf{g}}_{\mathbf{6}}(f_1,1),\\&\hat{g}_{7f\,1}=\hat{\mathbf{g}}_{\mathbf{7}}(f_1,1),\quad \hat{g}_{8f\,1}=\hat{\mathbf{g}}_{\mathbf{8}}(f_1,1),\\&Y_{5f\,1}=\mathbf{Y}(5,f_1),\quad Y_{6f\,1}=\mathbf{Y}(6,f_1),\\&Y_{5f\,2}=\mathbf{Y}(5,f_2),\quad Y_{6f\,2}=\mathbf{Y}(6,f_2)\end{aligned}\tag{32}$$

It should be noted that if the row of equation (28) which contains linear backward frequency is considered and frequencies other than linear backward frequency are neglected, equations similar to equations (30) to (32) are obtained while subscript f is replaced with b. Putting equation (25) into equation (30), one can extract the following formulation:

$$\begin{aligned}&D_0\eta_{3f\,1}=\lambda_f\,\eta_{3f\,1}+\left(q_{4f}\,a_f\,\bar{a}_f{}^2\right)\exp(-i\,\omega_f T_0)\\&+\left(-D_2a_f+q_{3f}\,a_f{}^2\bar{a}_f\right)\exp(i\,\omega_f T_0)\\&+q_{1f}\,a_f{}^3\exp(3i\,\omega_f T_0)+q_{2f}\,\bar{a}_f{}^3\exp(-3i\,\omega_f T_0)\end{aligned}\tag{33}$$

In order to obtain a finite particular solution for equation (33), it is necessary to put the coefficient of $\exp(i\,\omega_f T_0)$ equal to zero; then, putting $a_f=Q_f\exp(\alpha_f i)$ [68] and its derivative with respect to T_2 into obtained relation and some simplifications lead to the following results for Q_f and α_f:

$$\begin{aligned}&\alpha_f=\hat{q}_{3f}\,Q_f{}^2T_2+p_f,\quad \hat{q}_{3f}=-iq_{3f},\\&p_f=\text{const.},\quad Q_f=\text{const.}\end{aligned}\tag{34}$$

while Q_f and α_f are real terms related to T_2 [68] and q_{3f} is an imaginary term. Using equation (35), one can easily obtain the term of time response which is only related to linear forward frequency as shown in equation (36):

$$\begin{aligned}&w_1=\varepsilon w_{11}=\varepsilon\,\mathrm{a}_f\;\mathbf{Y}(5,f_1)\exp(\omega_f\,iT_0)\\&+\varepsilon\bar{a}_f\;\mathbf{Y}(5,f_2)\exp(-\omega_f\,iT_0)\end{aligned}\tag{35}$$

$$\begin{aligned}&\mathrm{w}_1=A_f\,\cos(\omega_f t+\frac{\hat{q}_{3f}\;\mathrm{A}_f{}^2}{4\left(|Y\;(5,f_1)|\right)^2}t+p_f+\delta),\\&\mathrm{A}_f=2\hat{Q}_f\;|Y\;(5,f_1)|,\hat{Q}_f=\varepsilon Q_f\end{aligned}\tag{36}$$

It should be noted that equation (36) is written by eliminating all linear frequencies other than linear forward frequency. According to equation (36), the nonlinear forward frequency ratio ($\omega_{NL(f)}/\omega_f$) can be written as shown in equation (37). In addition, considering the same procedure mentioned in equations (30) to (36), one can obtain a nonlinear backward frequency ratio ($\omega_{NL(b)}/\omega_b$) as shown in equation (37):

$$\begin{aligned}&\frac{\omega_{NL(f)}}{\omega_f}=1+\frac{e_f\;\mathrm{A}_f{}^2}{\omega_f},\quad \frac{\omega_{NL(b)}}{\omega_b}=1+\frac{e_b\;\mathrm{A}_b{}^2}{\omega_b},\\&e_f=\frac{\hat{q}_{3f}}{4\left(|Y\;(5,f_1)|\right)^2},e_b=\frac{\hat{q}_{3b}}{4\left(|Y\;(5,b_1)|\right)^2}\end{aligned}\tag{37}$$

In equation (37), the terms A_f and A_b denote amplitude parameters. In addition, e_f and e_b represent nonlinear forward and backward parameters. According to equation (37), one can elicit that the nonlinear forward frequency ratio is in direct linear relation with e_f inverse relation with ω_f, and direct relation with $A_f{}^2$. In addition, the nonlinear backward frequency ratio has direct relations with e_b and $A_b{}^2$ while its relation with linear backward frequency is inverse.

5. Results and Discussions

This paper investigates the nonlinear vibration of simply supported cross-ply laminated composite cylindrical shells surrounded by a nonlinear rotating elastic foundation. To ensure the correctness and validity of linear results of this study, the results of the literature can be compared with the results of this study. In this way, Table 1 compares the non-dimensional frequency parameter results of this study with literature for linear forward ($f_f{}^*=\omega_f R\sqrt{\rho/E_{22}}$) and linear backward ($f_b{}^*=\omega_b R\sqrt{\rho/E_{22}}$) waves of a laminated composite cross-ply cylindrical shell. The shell has a lamination scheme of $[0^o/90^o/0^o]$ while its material properties are: $\rho=1643\ \mathrm{kg/m^3}$, $E_{11}=19\ \mathrm{GPa}$, $E_{22}=7.6\ \mathrm{GPa}$, $G_{12}=4.1\ \mathrm{GPa}$, $\upsilon_{12}=0.26$ [67]. Furthermore, geometric characteristics of the considered cylindrical shell are: $h/R=0.006$ and $L/R=1$ while $m=1$ [67]. It should be noted that the difference rate is calculated by the following formulation:

$$\zeta=\left|\frac{\text{Present study response-reference response}}{\text{reference response}}\right|\times 100\tag{38}$$

Table 1 shows that for different values of circumferential wave number and also rotational velocity, the results of this study and reference [67] have good adaptation with each other while this adaptation for smaller values of circumferential wave number n is much better.

Table 1. Comparison of non-dimensional forward and backward frequency parameter results of this study with literature for different rotational speeds and circumferential wave numbers

Ω (rps)	n	Forward			Backward		
		Present	Reference [67]	difference rate	Present	Reference [67]	difference rate
0.1	1	1.061435	1.061140	0.03	1.061725	1.061429	0.03
	2	0.804409	0.803894	0.06	0.804729	0.804214	0.06
	3	0.599286	0.598187	0.18	0.599574	0.598476	0.18
	4	0.452513	0.450021	0.55	0.452761	0.450270	0.55
	5	0.350708	0.345149	1.61	0.350921	0.345363	1.61
	6	0.282392	0.270667	4.33	0.282577	0.270852	4.33
	7	0.240376	0.217489	10.52	0.240538	0.217651	10.52
1	1	1.060133	1.059836	0.03	1.063025	1.062728	0.03
	2	0.802978	0.802464	0.06	0.806181	0.805667	0.06
	3	0.598032	0.596937	0.18	0.600916	0.599820	0.18
	4	0.451513	0.449027	0.55	0.453999	0.451513	0.55
	5	0.350006	0.344459	1.61	0.352141	0.346593	1.60
	6	0.282043	0.270349	4.33	0.283891	0.272197	4.30
	7	0.240441	0.217651	10.47	0.242059	0.219269	10.39

In Table 2, the frequency results (Hz) of this study and reference [69] are presented for an isotropic non-rotating cylindrical shell on an elastic foundation with $m=1$. The geometric constants of the shell are considered to be $R=0.3015$ m, $L=0.41$ m, $h=1$ mm while the isotropic material constants are $E=210$ GPa, $\rho=7850$ kg/m^3 and $\upsilon=0.3$ [69]. According to Table 2, the results of this study and reference [69] demonstrate excellent agreement with each other.

Table 2. The frequency results of this study and literature for a non-rotating isotropic cylindrical shell surrounded by an elastic foundation

n	$K_w=0$ N/m^3, $K_p=1.5\times10^7$ N/m		$K_w=1.5\times10^7$ N/m^3, $K_p=2.5\times10^7$ N/m	
	Present	Ref. [69]	Present	Ref. [69]
3	2780.5951	2780.6	3487.4491	3487.5
4	3314.4768	3314.5	4233.7205	4233.7
5	3950.2596	3950.3	5077.1828	5077.2
6	4626.4943	4626.6	5959.9684	5960.1
7	5321.2712	5321.4	6861.4644	6861.6

After validation studies, in the rest of this paper, the effects of several parameters on the linear and nonlinear forward and backward frequency characteristics of laminated composite cross-ply rotating cylindrical shell on a nonlinear rotating elastic foundation are researched. In this way, a laminated composite rotating cylindrical shell is assumed with a lamination scheme of $[90^o/0^o/90^o]_s$ which rotates with $\Omega=35$ rad/s and is surrounded by a nonlinear rotating elastic foundation with $\Omega=35$ rad/s, $K_{NLw}=1.2\times10^{10}$ N/m^5, $K_{Lw}=1.2\times10^7$ N/m^3 and $K_p=1.2\times10^7$ N/m. It should be emphasized that the rotational velocities of the shell and foundation are the same. The shell is presumed to be from carbon fiber-reinforced polymeric (CFRP) material with $E_{11}=138.6$ GPa, $E_{22}=8.27$ GPa, $G_{12}=4.12$ GPa, $G_{23}=4.96$ GPa, $G_{13}=4.96$ GPa, $\rho=1824$ kg/m^3, $\upsilon_{12}=0.26$ and $\upsilon_{21}=E_{22}\upsilon_{12}/E_{11}$ [63] which has geometrical characteristics of $h=1$ mm, $L=0.8$ m, $R=1$ m. The results are attained for the mode shape of the cylindrical shell corresponds to $m=1$ and $n=4$. The mentioned constants and characteristics are assigned to obtain the whole results unless other values are noted.

Table 3 indicates the values of linear forward and backward frequencies as well as e_f, e_f/ω_f, e_b and e_b/ω_b for different values of the rotating foundation constants. According to this table, one can conclude that the values of linear forward and backward frequencies don't change for different values of K_{NLw}; the reason for this behavior is that the nonlinear constant of the foundation does not affect the values of stiffness, mass, and matrix $\mathbf{C}$ of the system. On the other hand, Table 3 shows that the values of e_f and e_b increas with an increase of K_{NLw}; because K_{NLw} is a nonlinear constant and its increment affects the nonlinear parameters of the system which are e_f and e_b. As represented in Table 3, the increase of e_f and e_b causes higher values for e_f/ω_f and e_b/ω_b, respectively. In addition to mentioned outcomes, Table 3 demonstrates the increase of the linear forward (backward) frequency and decrease of the nonlinear forward (backward) parameter with an increase of K_{Lw}

which leads to smaller values for e_f/ω_f (e_b/ω_b). The reason for the increase of the linear forward and backward frequencies with the increase of K_{Lw} is the increase in the system stiffness. Another result of Table 3 is that the increase of K_p leads to the increase of ω_f and ω_b which is due to the increase of the stiffness. Besides, Table 3 shows that nonlinear parameters (e_f and e_b) get smaller values with an increase of K_p. Table 3 illustrates that the increase of K_p results in the decrease of e_f/ω_f which is because of the increase of linear forward frequency and decrease of e_f. Furthermore, Table 3 demonstrates that the greater the value of K_p, the smaller the value of e_b/ω_b which can be justified by the increase of ω_b and decrease of e_b.

Figures 2 (a) and (b) show the effects of the nonlinear constant of the rotating elastic foundation (K_{NLw}) on the curves of nonlinear forward and backward frequency ratios against amplitude parameters, respectively. Figs. 2 (a) and (b) respectively show that for constant amplitude parameters, the increase of K_{NLw} leads to greater values for nonlinear forward and backward frequency ratios. This outcome is apparent because of the equation (37) as well as the results mentioned in Table 3 for different values of K_{NLw}. It can be seen that there is not a significant difference between the diagrams obtained for forward and backward waves because the matrix $\mathbf{C}$ which is the reason for the advent of forward and backward frequencies is small in comparison with K matrix.

Figures 3(a) and (b) depict the effects of K_{Lw} on the variation of nonlinear frequency ratios with amplitude parameters for forward and backward waves, respectively. Figs. 3(a) and (b) respectively illustrate that for constant values of amplitude parameters, as the value of K_{Lw} increases, the values of nonlinear forward and backward frequency ratios decrease. This outcome is because of the fact that, as shown in Table 3, the increase of K_{Lw} leads to smaller values for e_f/ω_f and e_b/ω_b which according to equation (37) leads to smaller values for nonlinear forward and backward frequency ratios, respectively.

The variations of nonlinear forward and backward frequency ratios with amplitude parameters for various K_p values are respectively illustrated in Figs. 4 (a) and (b). Figs. 4 (a) and (b) respectively show that for constant values of amplitude parameters, the increase of K_p value decreases the values of nonlinear frequency ratios for forward and backward waves.

These results are because of these facts that according to Table 3, the increase of K_p leads to smaller values for e_f/ω_f and e_b/ω_b. According to equation (37), for constants amplitude parameters, the smaller the values of e_f/ω_f and e_b/ω_b, the smaller the values of nonlinear forward and backward frequency ratios, respectively. Another outcome of Figs. 2 to 4 is that the increase of amplitude parameters causes greater values for nonlinear forward and backward frequency ratios; these results are in agreement with equation (37).

Table 3. The effect of the constants of the rotating elastic foundation on the vibration characteristics of the rotating cylindrical shell

Nonlinear foundation's constants $\times 10^{-7}$		ω_f (rad/s)	e_f (s.m^{-2})	e_f/ω_f (m^{-2})	ω_b (rad/s)	e_b (s.m^{-2})	e_b/ω_b (m^{-2})
	$K_{NLw}=0$ N/m^5	5934.00	4.5514415×10^5	76.70	5967.10	4.5533563×10^5	76.31
$K_{Lw}=1.2$ N/m^3	$K_{NLw}=600$N/m^5	5934.00	4.7961346×10^5	80.82	5967.10	4.7981523×10^5	80.41
$K_p=1.2$ N/m	$K_{NLw}=1200$ N/m^5	5934.00	5.0408278×10^5	84.95	5967.10	5.0429484×10^5	84.51
	$K_{NLw}=1800$ N/m^5	5934.00	5.2855209×10^5	89.07	5967.10	5.2877444×10^5	88.62
	$K_{Lw}=0$ N/m^3	5846.76	5.1166411×10^5	87.51	5879.83	5.1187576×10^5	87.06
$K_{NLw}=1200$ N/m^5	$K_{Lw}=0.6$ N/m^3	5890.54	5.0783148×10^5	86.21	5923.63	5.0804334×10^5	85.77
$K_p=1.2$ N/m	$K_{Lw}=1.2$ N/m^3	5934.00	5.0408278×10^5	84.95	5967.10	5.0429484×10^5	84.51
	$K_{Lw}=1.8$ N/m^3	5977.14	5.0041496×10^5	83.72	6010.26	5.0062723×10^5	83.30
	$K_p=0$ N/m	1700.48	1.75571525×10^6	1032.48	1732.47	1.75591500×10^6	1013.53
$K_{NLw}=1200$ N/m^5	$K_p=0.6$ N/m	4365.06	6.8626177×10^5	157.22	4397.59	6.8646757×10^5	156.10
$K_w=1.2$ N/m^3	$K_p=1.2$ N/m	5934.00	5.0408278×10^5	84.95	5967.10	5.0429484×10^5	84.51
	$K_p=1.8$ N/m	7165.31	4.1659305×10^5	58.14	7198.99	4.1681161×10^5	57.90

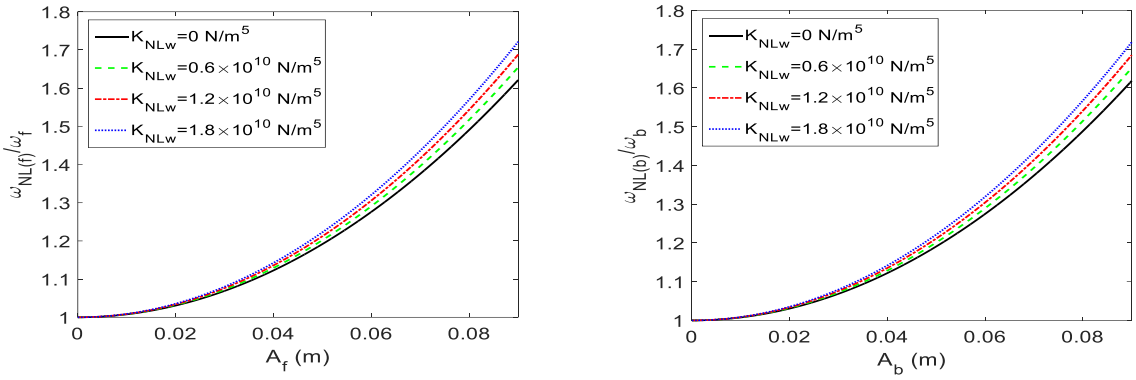

(a) (b)

Fig. 2. The effect of the elastic foundation nonlinear coefficient on the diagrams of, (a): nonlinear forward frequency ratio against amplitude parameter, (b): nonlinear backward frequency ratio versus amplitude parameter

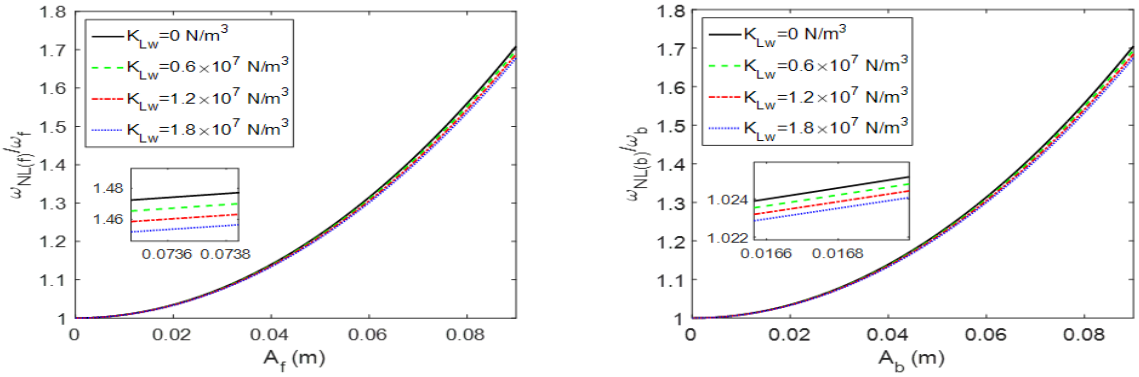

(a) (b)

Fig. 3. The effect of K_{Lw} on the curves obtained for, (a): nonlinear forward frequency ratio versus amplitude parameter, (b): nonlinear backward frequency ratio against amplitude parameter

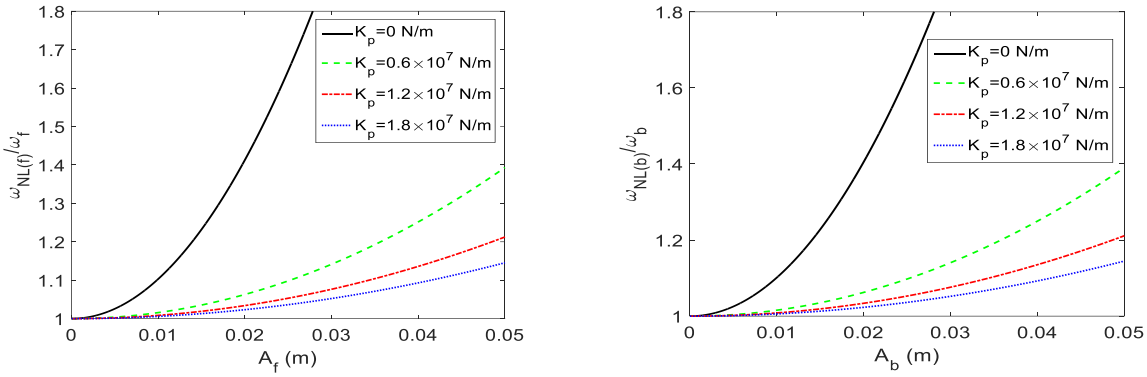

(a) (b)

Fig. 4. Diagrams of nonlinear frequency ratios versus amplitude parameters for different values of K_p for, (a): forward waves, (b): backward waves

Figures 5 (a) and (b) indicate the effects of the shell radius on the diagrams of nonlinear forward and backward frequency ratios versus amplitude parameters, respectively. Figs. 5 (a) and (b) indicate that for determining amplitude parameters, the greater the radius, the smaller the nonlinear frequency ratios for both forward and backward waves. In order to illustrate the reason for the results obtained from Figs. 5 (a) and (b), Table 4 and equation (37) can be used. Table 4 represents the effect of the shell radius on the linear forward and backward frequencies, nonlinear forward and backward parameters as well as e_f/ω_f and e_b/ω_b. This table shows that the values of linear frequencies and nonlinear parameters decrease with an increase in the radius. According to Table 4, the consequence of these reductions is the reduction of e_f/ω_f and e_b/ω_b which according to equation (37) leads to the reduction of forward and backward frequency ratios, respectively.

Figures 6 (a) and (b) represent the influence of the total thickness of the shell on the nonlinear frequency ratio to amplitude parameter curves for forward and backward waves, respectively. These figures illustrate that for constant amplitude parameters, the increase of the total thickness increases the values of $\omega_{NL(f)}/\omega_f$ and $\omega_{NL(b)}/\omega_b$. In order to explain the reason for this behavior, Table 5 can be utilized. Table 5 displays linear forward and backward frequencies, nonlinear forward and backward parameters as well as e_f/ω_f and e_f/ω_f for different values of the total thickness of the shell.

Table 5 shows that the increase of the total thickness results in the smaller linear forward and backward frequencies; the reason for this behavior could be the increase in the absolute values of the mass components of the shell. On the other hand, the values of the nonlinear forward and backward parameters increase as the total thickness increases. Table 5 indicates that the resultant decrease of ω_f (ω_b) and increase of e_f (e_b) is the increase of e_f/ω_f (e_b/ω_b) which according to equation (37) leads to an increase in the nonlinear forward (backward) frequency ratio.

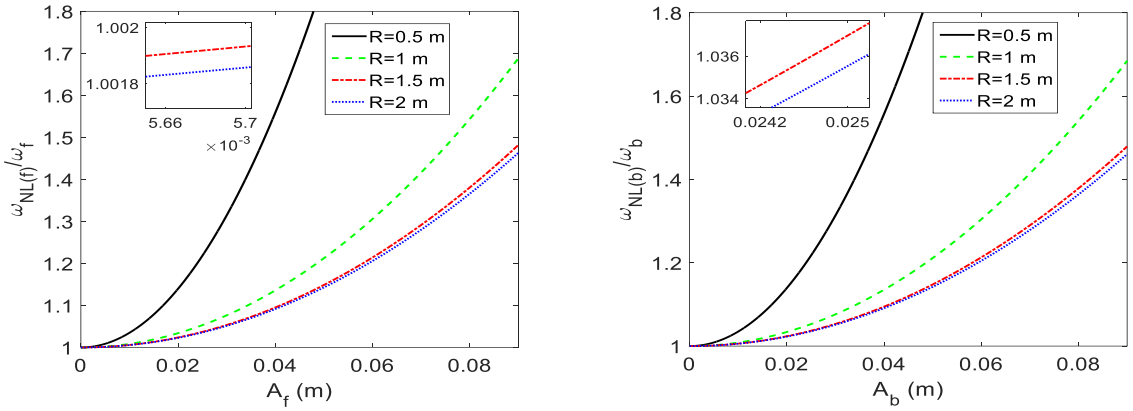

(a) (b)

Fig. 5. The effect of the cylindrical shell radius on the diagrams of nonlinear frequency ratios against amplitude parameters for, (a): forward waves, (b): backward waves

Table 4. The effects of the cylindrical shell radius on the vibration characteristics obtained for forward and backward waves

R (m)	ω_f (rad/s)	e_f (s.m^{-2})	e_f/ω_f (m^{-2})	ω_b (rad/s)	e_b (s.m^{-2})	e_b/ω_b (m^{-2})
0.5	9202.65	3.21413958×10^{6}	349.26	9236.13	3.21467500×10^{6}	348.05
1	5934.00	5.0408278×10^{5}	84.95	5967.10	5.0429484×10^{5}	84.51
1.5	5111.19	3.0399999×10^{5}	59.48	5143.62	3.0423795×10^{5}	59.15
2	4788.74	2.7373408×10^{5}	57.16	4820.26	2.7407214×10^{5}	56.86

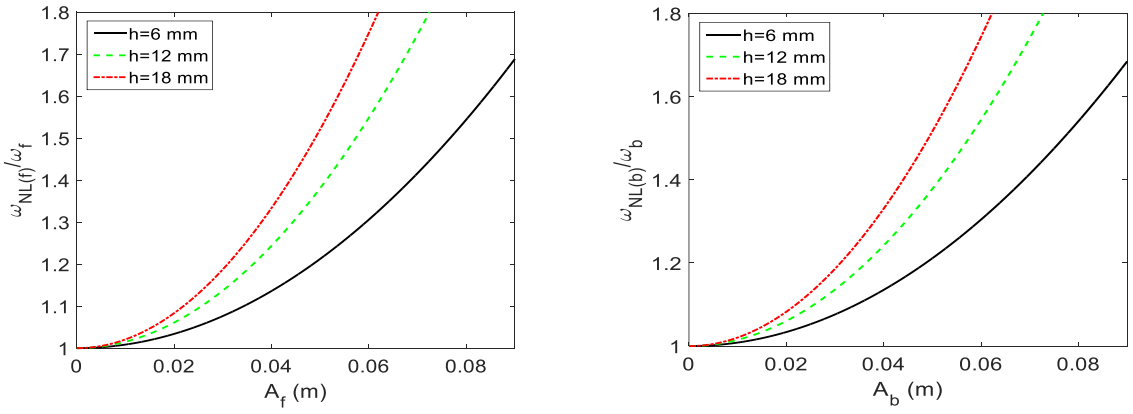

(a) (b)

Fig. 6. The impression of the total thickness of the shell on the nonlinear frequency ratio-amplitude parameter diagrams for, (a): forward waves, (b): backward waves

Table 5. The influence of the total thickness on the vibration characteristics

h (mm)	ω_f (rad/s)	e_f (s.m^{-2})	e_f/ω_f (m^{-2})	ω_b (rad/s)	e_b (s.m^{-2})	e_b/ω_b (m^{-2})
6	5934.00	5.0408278×10^5	84.95	5967.10	5.0429484×10^5	84.51
12	4325.76	6.5871650×10^5	152.28	4358.28	6.5891208×10^5	151.19
18	3666.09	7.6377340×10^5	208.33	3698.42	7.6396363×10^5	206.56

Figs. 7(a) and (b) demonstrate the impression of the length on the nonlinear frequency ratio versus amplitude parameter diagrams drawn for forward and backward waves, respectively. One can deduce from Fig. 7(a) that for a determined value of A_f, $\omega_{NL(f)}/\omega_f\big|_{L=0.4\text{ m}} > \omega_{NL(f)}/\omega_f\big|_{L=1.6\text{ m}} > \omega_{NL(f)}/\omega_f\big|_{L=1.2\text{ m}} > \omega_{NL(f)}/\omega_f\big|_{L=0.8\text{ m}}$. In a similar way, Fig. 7(b) indicates that for a determined amplitude parameter value, the outcome of $\omega_{NL(b)}/\omega_b\big|_{L=0.4\text{ m}} > \omega_{NL(b)}/\omega_b\big|_{L=1.6\text{ m}} > \omega_{NL(b)}/\omega_b\big|_{L=1.2\text{ m}} > \omega_{NL(b)}/\omega_b\big|_{L=0.8\text{ m}}$ is acquired. The reason for these outcomes can be clarified in Table 6. The influences of the length on the vibration characteristics including ω_f, e_f, e_f/ω_f, ω_b, e_b and e_b/ω_b are shown in Table 6. According to this table, one can conclude that linear frequencies for both forward and backward waves decrease with an increase of the length which is due to the increase of the absolute values of mass components. In addition, Table 6 shows that $e_f/\omega_f\big|_{L=0.4\text{ m}} > e_f/\omega_f\big|_{L=1.6\text{ m}} > e_f/\omega_f\big|_{L=1.2\text{ m}} > e_f/\omega_f\big|_{L=0.8\text{ m}}$ and $e_b/\omega_b\big|_{L=0.4\text{ m}} > e_b/\omega_b\big|_{L=1.6\text{ m}} > e_b/\omega_b\big|_{L=1.2\text{ m}} > e_b/\omega_b\big|_{L=0.8\text{ m}}$; the reason for these results is that depending on the rate of the changes of e_f (e_b) and ω_f (ω_b), e_f/ω_f (e_b/ω_b) increases or decreases which according to equation (37) affects the value of nonlinear forward (backward) frequency ratio.

Figures 8 (a) and (b) respectively display diagrams of $\omega_{NL(f)}/\omega_f$ - A_f and $\omega_{NL(b)}/\omega_b$ - A_b for different values of the rotation speed of the laminated composite cross-ply cylindrical shell on a nonlinear rotating elastic foundation. Figs. 8 (a) and (b) show that for constant amplitude parameters, rotational velocity causes a small and negligible difference in the forward and backward frequency ratio values. Table 7 demonstrates the effects of the rotation speed on the vibration characteristics of the cylindrical shell. This table shows that the values of linear frequencies as well as e_f/ω_f and e_b/ω_b are not significantly affected by the change of Ω which justifies the behavior of the curves of Figs. 8 (a) and (b).

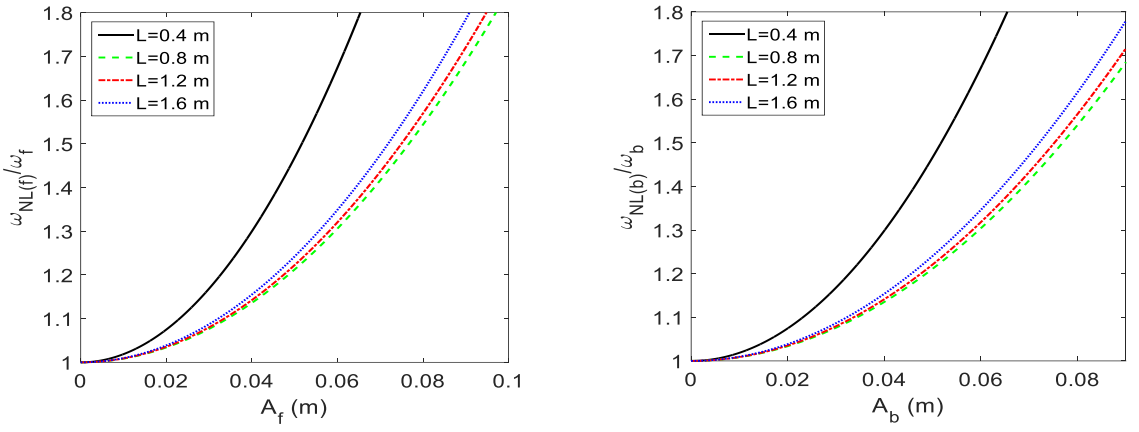

Fig. 7. The influence of the rotating shell length on the curves of, (a): nonlinear forward frequency ratio, (b): nonlinear backward frequency ratio, versus amplitude parameter

Table 6. Vibration characteristics of the rotating cylindrical shells with different length values

L (m)	ω_f (rad/s)	e_f (sm^{-2})	e_f/ω_f (m^{-2})	ω_b (rad/s)	e_b (sm^{-2})	e_b/ω_b (m^{-2})
0.4	9439.31	1.76724657×10^6	187.22	9470.73	1.76831396×10^6	186.71
0.8	5934.00	5.0408278×10^5	84.95	5967.10	5.0429484×10^5	84.51
1.2	5024.14	4.4698669×10^5	88.97	5057.55	4.4714929×10^5	88.41
1.6	4664.90	4.5191660×10^5	96.88	4698.40	4.5206975×10^5	96.22

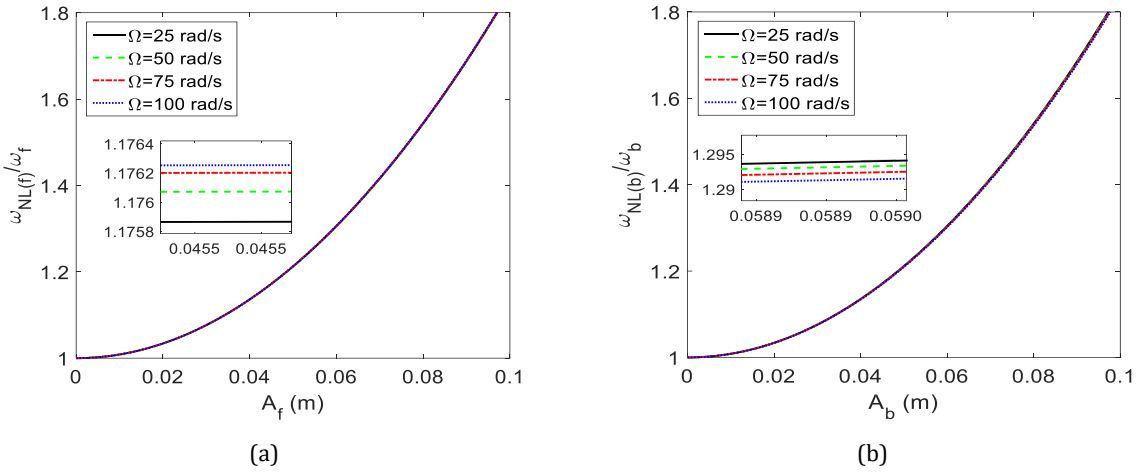

(a) (b)

Fig. 8. The images of the diagrams of nonlinear frequency ratios against amplitude parameters acquired for different rotational speeds for, (a): forward waves, (b): backward waves

Table 7. The impression of rotational velocity on the vibration characteristics of the rotating cylindrical shell

Ω (rad/s)	ω_f (rad/s)	e_f (s.m^{-2})	e_f/ω_f (m^{-2})	ω_b (rad/s)	e_b (s.m^{-2})	e_b/ω_b (m^{-2})
25	5938.11	5.0416784×10^5	84.90	5961.75	5.0431931×10^5	84.59
50	5928.23	5.0392101×10^5	85.00	5975.51	5.0422395×10^5	84.38
75	5919.63	5.0356049×10^5	85.07	5990.57	5.0401490×10^5	84.13
100	5912.33	5.0308684×10^5	85.09	6006.92	5.0369272×10^5	83.85

Another consequence of Figs. 5 to 8 is the fact that the greater the amplitude parameters, the greater the nonlinear forward and backward frequency ratios; the mentioned outcome is in agreement with equation (37).

6. Conclusions

In this study, nonlinear vibration responses of rotating laminated composite cross-ply cylindrical shell surrounded by a nonlinear rotating elastic foundation are presented by applying modal analysis and multiple scales method to the nonlinear equation of the system in the state space form. The system is modeled considering von Karman's nonlinear theory while FSDT and rotary inertia are taken into consideration. The influences of initial hoop tension, as well as centrifugal and Coriolis accelerations in the rotating cylindrical shell modeling are taken into account. The relation of the rotating elastic foundation which surrounds the shell is obtained with the Winkler-Pasternak model. The nonlinear ordinary differential equation of the rotating shell is derived via the Ritz method and then is converted to the state space form. Afterward, modal analysis and multiple scales method are utilized to obtain nonlinear frequency ratios for forward and backward waves. The results published in the literature are used to investigate the validity of the results of this study and good agreement is observed. The effects of several parameters including the nonlinear and linear constants of elastic foundation, radius, total thickness, length and rotation speed on the linear and nonlinear vibration behavior are presented which can be classified as follows:

1. For determined amplitude parameters, the greater the nonlinear constant of the rotating elastic foundation, the greater the nonlinear forward (backward) frequency ratio; the reason for this conclusion is the increase of the nonlinear forward (backward) parameter of the system.
2. The increase of the nonlinear constant of the rotating elastic foundation doesn't have any effect on the linear forward and backward frequencies.
3. The increase of the rotating foundation linear constants leads to the increase of the stiffness and thus the increase of linear frequencies. The increase of the linear frequencies along with the decrease of the nonlinear parameters caused by the increase of the rotating foundation linear constants leads to the decrease of the nonlinear frequency ratios.
4. The linear forward and backward frequencies get smaller values with an

increase in the radius. In addition, the increase of the radius leads to smaller nonlinear parameters and nonlinear frequency ratios for both forward and backward waves.

5. As the total thickness of the rotating cylindrical shell increases, the absolute values of the mass components of the system become higher which leads to the decrease of the values of the linear frequencies. Furthermore, the decrease of the linear frequencies along with the increase of the nonlinear parameters which are the results of the increase of the total thickness cause greater values for nonlinear frequency ratios.
6. The increase of the absolute values of mass components due to the increase of the length leads to the reduction of the values of linear forward and backward frequencies.
7. The influences of the rotation speed on the linear frequencies and nonlinear frequency ratios are not remarkable and can be ignored.
8. The increase of the amplitude parameters leads to the increase of the nonlinear forward and backward frequency ratios.

References

[1] Rao, S.S., 2011. *Mechanical vibrations*. fifth edition. Prentice Hall.

[2] Sofiyev, A.H. and Aksogan, O., 2003. Non-linear free vibration analysis of laminated non-homogeneous orthotropic cylindrical shells. *Proceedings of the Institution of Mechanical Engineers, Part K: Journal of Multi-Body Dynamics*, *217*(4), pp.293-300.

[3] Sofiyev, A.H., Keskin, S.N. and Sofiyev, A.H., 2004. Effects of elastic foundation on the vibration of laminated non-homogeneous orthotropic circular cylindrical shells. *Shock and Vibration*, *11*(2), pp.89-101.

[4] Najafov, A.M., Sofiyev, A.H., Hui, D., Kadioglu, F., Dorofeyskaya, N.V. and Huang, H., 2014. Non-linear dynamic analysis of symmetric and antisymmetric cross-ply laminated orthotropic thin shells. *Meccanica*, *49*(2), pp.413-427.

[5] Arshid, E., Amir, S. and Loghman, A., 2016. Bending and buckling behaviors of heterogeneous temperature-dependent micro annular/circular porous sandwich plates integrated by FGPEM nano-Composite layers. *Journal of Sandwich Structures & Materials*, 1099636220955027.

[6] Arshid, E. and Khorshidvand, A.R., 2018. Free vibration analysis of saturated porous FG circular plates integrated with piezoelectric actuators via differential quadrature method. *Thin-Walled Structures*, *125*, pp.220-233.

[7] Mohammadimehr, M., Arshid, E., Alhosseini, S.M.A.R., Amir, S. and Arani, M.R.G., 2019. Free vibration analysis of thick cylindrical MEE composite shells reinforced CNTs with temperature-dependent properties resting on viscoelastic foundation. *Structural Engineering and Mechanics*, *70*(6), pp.683-702.

[8] Babaei, A. and Yang, C.X., 2019. Vibration analysis of rotating rods based on the nonlocal elasticity theory and coupled displacement field. *Microsystem Technologies*, *25*(3), pp.1077-1085.

[9] Sofiyev, A.H., 2019. Review of research on the vibration and buckling of the FGM conical shells. *Composite Structures*, *211*, pp.301-317.

[10] Babaei, A., Parker, J. and Moshaver, P., 2020. Energy Resource for a RFID System Based on Dynamic Features of Reddy-Levinson Beam. In *ASME International Mechanical Engineering Congress and Exposition* (Vol. 84553, p. V07BT07A045). American Society of Mechanical Engineers.

[11] Rahmani, A., Babaei, A. and Faroughi, S., 2020. Vibration characteristics of functionally graded micro-beam carrying an attached mass. *Mechanics of Advanced Composite Structures*, *7*(1), pp.49-58.

[12] Avey, M. and Yusufoglu, E., 2020. On the solution of large-amplitude vibration of carbon nanotube-based double-curved shallow shells. *Mathematical Methods in the Applied Sciences*.

[13] Arshid, E., Arshid, H., Amir, S. and Mousavi, S.B., 2021. Free vibration and buckling analyses of FG porous sandwich curved microbeams in thermal environment under magnetic field based on modified couple stress theory. *Archives of Civil and Mechanical Engineering*, *21*(1), pp.1-23.

[14] Khorasani, M., Soleimani-Javid, Z., Arshid, E., Lampani, L. and Civalek, Ö., 2021. Thermo-elastic buckling of honeycomb micro plates integrated with FG-GNPs reinforced Epoxy skins with stretching effect. *Composite Structures*, *258*, 113430.

[15] Arshid, E. and Amir, S., 2021. Size-dependent vibration analysis of fluid-infiltrated porous curved microbeams integrated with reinforced functionally graded graphene platelets face sheets considering thickness stretching effect. *Proceedings of the Institution of Mechanical Engineers, Part L: Journal of Materials: Design and Applications*, *235*(5), pp.1077-1099.

[16] Mousavi, S.B., Amir, S., Jafari, A. and Arshid, E., 2021. Analytical solution for analyzing initial curvature effect on vibrational behavior of PM beams integrated with FGP layers based on trigonometric theories. *Advances in nano research*, *10*(3), pp.235-251.

[17] Arshid, E., Amir, S. and Loghman, A., 2021. Thermal buckling analysis of FG graphene nanoplatelets reinforced porous nanocomposite MCST-based annular/circular microplates. *Aerospace Science and Technology*, *111*, 106561.

[18] Amir, S., Soleimani-Javid, Z. and Arshid, E., 2019. Size-dependent free vibration of sandwich micro beam with porous core subjected to thermal load based on SSDBT. *ZAMM-Journal of Applied Mathematics and Mechanics/Zeitschrift für Angewandte Mathematik und Mechanik*, *99*(9), e201800334.

[19] Amir, S., Arshid, E. and Arani, M.R.G., 2019. Size-dependent magneto-electro-elastic vibration analysis of FG saturated porous annular/circular micro sandwich plates embedded with nano-composite face sheets subjected to multi-physical pre loads. *Smart Structures and Systems*, *23*(5), pp.429-447.

[20] Amir, S., Arshid, E., Rasti-Alhosseini, S.A. and Loghman, A., 2020. Quasi-3D tangential shear deformation theory for size-dependent free vibration analysis of three-layered FG porous micro rectangular plate integrated by nano-composite faces in hygrothermal environment. *Journal of Thermal Stresses*, *43*(2), pp.133-156.

[21] Amir, S., Vossough, A.R., Vossough, H. and Arshid, E., 2020. Nonlinear Magneto-Nonlocal Vibration Analysis of Coupled Piezoelectric Micro-Plates Reinforced with Agglomerated CNTs. *Mechanics of Advanced Composite Structures*, *7*(1), pp.109-119.

[22] Amir, S., Arshid, E., Khoddami Maraghi, Z., Loghman, A. and Ghorbanpour Arani, A., 2020. Vibration analysis of magnetorheological fluid circular sandwich plates with magnetostrictive facesheets exposed to monotonic magnetic field located on visco-Pasternak substrate. *Journal of Vibration and Control*, *26*(17-18), pp.1523-1537.

[23] Amir, S., Arshid, E. and Maraghi, Z.K., 2020. Free vibration analysis of magneto-rheological smart annular three-layered plates subjected to magnetic field in viscoelastic medium. *Smart Structures and Systems*, *25*(5), pp.581-592.

[24] Arshid, E., Kiani, A., Amir, S. and Zarghami Dehaghani, M., 2019. Asymmetric free vibration analysis of first-order shear deformable functionally graded magneto-electro-thermo-elastic circular plates. *Proceedings of the Institution of Mechanical Engineers, Part C: Journal of Mechanical Engineering Science*, *233*(16), pp.5659-5675.

[25] Arshid, E., Khorshidvand, A.R. and Khorsandijou, S.M., 2019. The effect of porosity on free vibration of SPFG circular plates resting on visco-Pasternak elastic foundation based on CPT, FSDT and TSDT. *Structural Engineering and Mechanics*, *70*(1), pp.97-112.

[26] Arshid, E., Kiani, A. and Amir, S., 2019. Magneto-electro-elastic vibration of moderately thick FG annular plates subjected to multi physical loads in thermal environment using GDQ method by considering neutral surface. *Proceedings of the Institution of Mechanical Engineers, Part L: Journal of Materials: Design and Applications*, *233*(10), pp.2140-2159.

[27] Arshid, E., Khorasani, M., Soleimani-Javid, Z., Amir, S. and Tounsi, A., 2021. Porosity-dependent vibration analysis of FG microplates embedded by polymeric nanocomposite patches considering hygrothermal effect via an innovative plate theory. *Engineering with Computers*, 1-22.

[28] Babaei, A., 2021. Forced vibrations of size-dependent rods subjected to: impulse, step, and ramp excitations. *Archive of Applied Mechanics*, 1-13.

[29] Babaei, A., 2021. Forced vibration analysis of non-local strain gradient rod subjected to harmonic excitations. *Microsystem Technologies*, *27*(3), pp.821-831.

[30] SafarPour, H., Ghanbari, B. and Ghadiri, M., 2019. Buckling and free vibration analysis of high speed rotating carbon nanotube reinforced cylindrical piezoelectric shell. *Applied Mathematical Modelling*, *65*, pp.428-442.

[31] Lam, K.Y. and Loy, C.T., 1995. Analysis of rotating laminated cylindrical shells by different thin shell theories. *Journal of Sound and Vibration*, *186*(1), pp.23-35.

[32] Lam, K.Y. and Loy, C. T., 1998. Influence of boundary conditions for a thin laminated rotating cylindrical shell. *Composite structures*, *41*(3-4), pp.215-228.

[33] Zhao, X., Liew, K.M. and Ng, T.Y., 2002. Vibrations of rotating cross-ply laminated circular cylindrical shells with stringer and ring stiffeners. *International Journal of Solids and Structures*, *39*(2), pp.529-545.

[34] Civalek, Ö., 2007. A parametric study of the free vibration analysis of rotating laminated cylindrical shells using the method of discrete singular convolution. *Thin-Walled Structures*, *45*(7-8), pp.692-698.

[35] Civalek, Ö. and Gürses, M., 2009. Free vibration analysis of rotating cylindrical shells using discrete singular convolution technique. *International Journal of Pressure Vessels and Piping*, *86*(10), pp.677-683.

[36] Sun, S., Chu, S. and Cao, D., 2012. Vibration characteristics of thin rotating cylindrical shells with various boundary conditions. *Journal of Sound and Vibration*, *331*(18), pp.4170-4186.

[37] Hussain, M., Naeem, M.N., Shahzad, A., He, M.G. and Habib, S., 2018. Vibrations of rotating cylindrical shells with functionally graded material using wave propagation approach. *Proceedings of the Institution of Mechanical Engineers, Part C: Journal of Mechanical Engineering Science*, *232*(23), pp.4342-4356.

[38] Ghasemi, A.R. and Meskini, M., 2019. Free vibration analysis of porous laminated rotating circular cylindrical shells. *Journal of Vibration and Control*, *25*(18), pp.2494-2508.

[39] Mohammadrezazadeh, S. and Jafari, A.A., 2019. The influences of magnetostrictive layers on active vibration control of laminated composite rotating cylindrical shells based on first-order shear deformation theory. *Proceedings of the Institution of Mechanical Engineers, Part C: Journal of Mechanical Engineering Science*, *233*(13), pp.4606-4619.

[40] Ghasemi, A.R. and Mohandes, M., 2019. Free vibration analysis of rotating fiber–metal laminate circular cylindrical shells. *Journal of Sandwich Structures & Materials*, *21*(3), pp.1009-1031.

[41] Mohammadrezazadeh, S. and Jafari, A.A., 2020. Active control of free and forced vibration of rotating laminated composite cylindrical shells embedded with magnetostrictive layers based on classical shell theory. *Mechanics of Advanced Composite Structures*, 7, pp.355-369.

[42] Emam, S.A., 2002. *A Theoretical and Experimental Study of Nonlinear Dynamics of Buckled Beams*. PhD Thesis, Virginia Polytechnic Institute, Virginia.

[43] Young-Shin, L. and Young-Wann, K., 1999. Nonlinear free vibration analysis of rotating hybrid cylindrical shells. *Computers & structures*, *70*(2), pp.161-168.

[44] Liu, Y. and Chu, F., 2012. Nonlinear vibrations of rotating thin circular cylindrical shell. *Nonlinear Dynamics*, *67*(2), pp.1467-1479.

[45] Wang, Y.Q., 2014. Nonlinear vibration of a rotating laminated composite circular cylindrical shell: traveling wave vibration. *Nonlinear Dynamics*, *77*(4), pp.1693-1707.

[46] Dong, Y.H., Zhu, B., Wang, Y., Li, Y.H. and Yang, J., 2018. Nonlinear free vibration of graded graphene reinforced cylindrical shells: Effects of spinning motion and axial load. *Journal of Sound and Vibration*, *437*, pp.79-96.

[47] Sun, S., Liu, L. and Cao, D., 2018. Nonlinear travelling wave vibrations of a rotating thin cylindrical shell. *Journal of Sound and Vibration*, *431*, pp.122-136.

[48] Yao, M., Niu, Y. and Hao, Y., 2019. Nonlinear dynamic responses of rotating pretwisted cylindrical shells. *Nonlinear Dynamics*, *95*(1), pp.151-174.

[49] Rostami, R., Mohamadimehr, M. and Rahaghi, M. I., 2019. Dynamic stability and nonlinear vibration of rotating sandwich cylindrical shell with considering FG core integrated with sensor and actuator. *Steel and Composite Structures*, *32*(2), pp.225-237.

[50] Liu, T., Zhang, W., Mao, J.J. and Zheng, Y., 2019. Nonlinear breathing vibrations of eccentric rotating composite laminated circular cylindrical shell subjected to temperature, rotating speed and external excitations. *Mechanical Systems and Signal Processing*, *127*, pp.463-498.

[51] Du, D., Sun, W., Yan, X. and Xu, K., 2020. Nonlinear vibration analysis of the rotating hard-coating cylindrical shell based on the

domain decomposition method. *Thin-Walled Structures*, 107236.

[52] Li, C., Li, P., Zhong, B. and Miao, X., 2020. Large-amplitude vibrations of thin-walled rotating laminated composite cylindrical shell with arbitrary boundary conditions. *Thin-Walled Structures*, *156*, 106966.

[53] Sofiyev, A. H. and Schnack, E., 2012. The vibration analysis of FGM truncated conical shells resting on two-parameter elastic foundations. *Mechanics of Advanced Materials and Structures*, *19*(4), pp.241-249.

[54] Pasternak, P.L., 1954. On a new method of analysis of an elastic foundation by means of two foundation constants, Gos. Izd. Lit. po Stroit I Arkh. Moscow, USSR.

[55] Kerr A.D., 1964 , Elastic and visco-elastic foundationmodels, J. Appl.Mech., vol. 31, pp. 491–498.

[56] Sofiyev, A.H. and Kuruoglu, N., 2017. Combined effects of transverse shear stresses and nonlinear elastic foundations on the nonlinear dynamic response of heterogeneous orthotropic cylindrical shells. *Composite Structures*, *166*, pp.153-162.

[57] Sheng, G.G., Wang, X., Fu, G. and Hu, H., 2014. The nonlinear vibrations of functionally graded cylindrical shells surrounded by an elastic foundation. *Nonlinear Dynamics*, *78*(2), pp.1421-1434.

[58] Sofiyev, A.H., 2016. Large amplitude vibration of FGM orthotropic cylindrical shells interacting with the nonlinear Winkler elastic foundation. *Composites Part B: Engineering*, *98*, pp.141-150.

[59] Sofiyev, A.H., Karaca, Z. and Zerin, Z., 2017. Non-linear vibration of composite orthotropic cylindrical shells on the non-linear elastic foundations within the shear deformation theory. *composite structures*, *159*, pp.53-62.

[60] Hadi, A., Ovesy, H.R., Shakhesi, S. and Fazilati, J., 2017. Large amplitude dynamic analysis of FGM cylindrical shells on nonlinear elastic foundation under thermomechanical loads. *International Journal of Applied Mechanics*, *9*(07), 1750105.

[61] Babaei, H., Kiani, Y. and Eslami, M.R., 2019. Large amplitude free vibrations of long FGM cylindrical panels on nonlinear elastic foundation based on physical neutral surface. *Composite Structures*, *220*, pp.888-898.

[62] Rao, S.S., 2007. *Vibration of Continuous Systems*. JOHN WILEY & SONS, INC.

[63] Reddy, J.N., 2004. *Mechanics of laminated composite plates and shells: theory and analysis*. Second Edition, CRC Press.

[64] Reddy, J.N., 2002. *Energy principles and variational methods in applied mechanics*. John Wiley &Sons.

[65] Talebitooti, M., 2013. Three-dimensional free vibration analysis of rotating laminated conical shells: layerwise differential quadrature (LW-DQ) method. *Archive of Applied Mechanics*, *83*(5), pp.765-781.

[66] Qatu, M.S., 2004. *Vibration of laminated shells and plates*. Elsevier.

[67] Li H., Lam K.Y. and Ng T.Y., 2005. *Rotating shell dynamics*. (Vol. 50), Elsevier.

[68] Nayfeh, A.H and Mook, D.T., 1995. *Nonlinear Oscillations*. John Wiley & Sons, Inc.

[69] Shah, A.G., Mahmood, T., Naeem, M.N. and Arshad, S.H., 2011. Vibration characteristics of fluid-filled cylindrical shells based on elastic foundations. *Acta mechanica*, *216*(1-4), pp.17-28.